

The effect of bottom substrate on inherent optical properties: Evidence of biogeochemical processes

Emmanuel Boss

School of Marine Sciences, University of Maine, Orono, Maine 04469

J. Ronald V. Zaneveld

College of Ocean and Atmospheric Sciences, Oregon State University, Corvallis, Oregon 97331

Abstract

Measurements of inherent optical properties (IOP) were conducted over bottoms with different substrates by use of a sampling package mounted on and operated by a SCUBA diver. It was found that in areas of low ambient currents the distribution of IOP varies with bottom type in (1) its value relative to a nearby bottom of different type, (2) its vertical gradient, and (3) its variability. This implies that radiative transfer modeling in shallow environments may need to include, besides the bottom characteristics, the bottom effect on in-water IOP. In tidally flushed shallow banks, vertical and horizontal gradients over scales of O(1, 10 m), respectively, are as large as temporal gradients over scales of minutes and cannot be separated in our measurements. However, bottom-substrate-related processes over the banks result in gradients over large horizontal spatial scales and tidal timescales. The distribution of IOP is consistent with several biogeochemical processes that may be active at a given bottom substrate and suggest that optical measurements may provide a useful tool to infer and quantify bulk rates of biogeochemical processes.

The classic *forward* problem in ocean optics is the calculation of the distribution of radiance in space given the optical properties of the medium (the inherent optical properties [IOP]; Preisendorfer 1976) and appropriate boundary conditions. To solve this “forward” problem, we need to know the details of the light source or sources (e.g., the solar spectrum and its direct and diffuse light just above the ocean), transmission through the boundaries of the domain (e.g., a wave-modulated air-ocean interface), and the optical properties of the medium. In the ocean, photons interact with the water molecules and with dissolved and particulate material within the water. These constituents determine the IOP of any given water mass. In shallow waters, an additional complexity comes from the existence of a bottom boundary, which interacts with light (through absorption and reflection).

The forward problem is of importance for interpretation of remotely sensed ocean color in shallow areas (e.g., Lee et al. 1999; Carder et al. 2003) and for systems designed to image the bottom (e.g., for classification of bottom substrate and target recognition; McLean et al. 1995). In order to understand the distribution of IOP in space and time, we need to understand their relationship to processes occurring in the ocean as well as processes associated with the bottom.

The ocean bottom affects light propagation not only through its own optical properties; the bottom substrate and

the organisms living within and above it may exert an influence on the optical properties of the water overlying the bottom. This influence of bottom substrate (and biogeochemical processes associated with it) on the water IOP is the subject of this article.

The process most studied with respect to the influence of substrate on water-column IOP is sediment resuspension. Bottom stress due to currents and waves interacting with the bottom substrate causes resuspension of sediment material into the water column (e.g., Middleton and Southard 1984; Abelson et al. 1993). In principle, the optical properties of the bottom sediment (index of refraction of particles, shape, and size distribution), its physical properties (density and shape), magnitude of bottom stress, and resuspension history determine the sediment load and its contribution to the water-column IOPs. Recent studies of sediment resuspension near reefs and its optical signature have been reported by Lacombe et al. (1995), Lacombe and Woolfe (1999), and Heap et al. (1999).

There are, however, other biogeochemical processes that influence near-bottom optical properties:

1. Diffusive and advective (when sediment is resuspended) flux of colored dissolved material released from sediment pore water (e.g., Boss et al. 2001a).
2. Removal of selected particulate material from the water column by benthic filter feeders such as corals and sponges (e.g., Yahel et al. 1998).
3. Emergence of organisms (“particulate material”) from the sediment into the water column (e.g., Dagg 1997).
4. Mechanical resuspension of sediment by benthic organisms and water column organisms such as fish (Yahel et al. unpubl. data).
5. Release of colored particulate and dissolved waste products into the water by in-water organisms such as zooplankton and fish and by release of dissolved waste prod-

Acknowledgments

This research was sponsored by the Coastal Benthic Optical Properties initiative of the Office of Naval Research. We thank R. Wheatcroft for providing us his current velocity measurements. Discussions with R. Zimmerman and D. Burdige initiated the pore-water sampling. We thank P. Hill for an insightful review of an earlier version of this manuscript and J. Washburn and F. Baratange for assistance in sampling and in designing the diver package.

ucts by bottom-dwelling organisms such as coral and sponges.

In the present article, we demonstrate that near-bottom IOP can be influenced by such biogeochemical processes. We refer the readers to the book edited by Z. Dubinski (1990) for in-depth reviews of biogeochemical processes near coral reefs.

The use of optics to infer the contribution of biogeochemical processes has advantages as well as disadvantages; the advantage of optical measurements to quantify biogeochemical processes and parameters is that they can be performed in situ and are noninvasive, an advantage relative to laboratory sample analysis techniques. The disadvantage is that only the net effect of all processes present is measured.

Measurements of IOP close to the bottom (at <1 m above the bottom) have almost always been associated with studies of sediment dynamics (e.g., Pak 1983). Near-bottom measurements of IOP other than optical back-scattering or beam attenuation at a single wavelength are almost nonexistent (exceptions include the chlorophyll fluorescence measurements of Frechette et al. 1989, obtained by use of moorings). In this article, we present spectral absorption and beam-attenuation data collected at distances of tens of centimeters above the bottom by use of a sampling system mounted on a SCUBA diver.

Horizontal gradients in dissolved and particulate material have been observed between reefs and the adjacent ocean and were linked to the reef community metabolism (Erez 1990). A diurnal cycle in resuspension of particulate matter has been documented near reefs (Heap et al. 1999; Yahel et al. 2002). Although Heap et al. (1999) suggested that vertical migration of zooplankton was the likely cause for their observation, Yahel et al. (2002) found a direct link between sediment resuspension and fish activity. Horizontal gradients in phytoplankton pigment between reefs and adjacent waters were reported by Yahel et al. (1998).

The main focus of this article is to show, and quantify in terms of net effect on IOPs, the influence of biogeochemical processes on the IOP distribution in the vicinity of the bottom on horizontal scales of tens of meters, vertical scales of tens of centimeters, and temporal scales of minutes. In certain cases, the IOP distribution could be used to quantify the rate of these processes (the *inverse* problem).

Materials and methods

We have described (Zaneveld et al. 2001) the physical-optical diving package with which we sampled. In short, absorption and attenuation at nine wavelengths in the visible spectrum and conductivity, temperature, and depth (CTD) were measured by an apparatus mounted on the back of a SCUBA diver. Water for measurements in the package is pumped through a hose whose intake is at the diver's hand. By use of a 0.2- μm filter, we obtained the absorption by the dissolved fraction (denoted by a subscript *g*). Subtracting the measurement with the filter from the measurement without the filter (denoted by subscript *pg* for particulate and dissolved), the particulate fraction is obtained (denoted by a subscript *p*).

The measurements described here were obtained in areas adjacent to Lee Stocking Island (LSI), Bahamas (Fig. 1). The sampling sites included (Fig. 1)

Channel Marker (CM): 2–6 m depth with bottom sediment containing carbonate ooids and seagrass cover ranging from dense to none.

Rainbow Garden (RG): Bottom varying from seagrass (4.5–9 m depth) to sand to a reef containing macroalgae, sponges, and corals (1–4.5 m depth).

Rainbow South (RS): Tidal channel (2–7 m depth) with a clear carbonate sediment bottom.

Horseshoe Reef (HS): Sand flats (10–11 m depth) adjacent to a reef containing macroalgae, sponges, and corals (8–10 m depth).

South Perry Reef (SP): Sand flats (15–16 m depth) adjacent to a reef containing macroalgae, sponges, and corals (7–15 m depth).

North Perry Reef (NP): Sand flats (15–16 m depth) adjacent to a reef containing macroalgae, sponges, and corals (11–15 m depth).

The first three sites are shallow channels where large volumes of water are exchanged tidally between Exuma Sound to the southeast and the Bahamas banks, which results in swift currents. The latter three sites were located on the Exuma Sound side of LSI and experienced much weaker currents (see below).

Our study is focused on variability at small temporal and spatial scales [scales of $O(10)$ min and $O(10)$ m] and its relationship to the processes associated with the bottom substrate. The large temporal and spatial scales (e.g., advective tidal fluxes) provide the background above which our observations need to be evaluated.

We reference depth to the bottom, because this is the primary length of importance when dealing with benthic processes. Other important vertical length scales are distance from surface (important for wave effects) and stratification depth $(-1/\rho_o d\rho/dz)^{-1}$.

We denote by “horizontal gradients” the differences between measurements carried out above two adjacent and different substrates, even though they each were at different depths. The maximum depth difference was as high as 9 m (SP). For the 12 sections carried out in 2000 (Table 1, when CTD data was available) the density gradients between the two substrates were $\Delta\sigma < 0.015 \text{ kg m}^{-3}$. For 9 of the 12 $\Delta\sigma < 0.01 \text{ kg m}^{-3}$, which is less than criteria used elsewhere to estimate an actively mixing layer depth (Brainerd and Gregg 1995). It is most often the case in Exuma Sound that the mixed layer depth is >20 m and thus encompasses the reef and adjacent sand flats within it (Hickey et al. 2000). This suggests that the observed gradients between properties above different substrates are not aliased significantly by vertical gradients.

Sampling periods—The measurements described here span three sampling periods, spring 1999 and winter and spring 2000. Each sampling period lasted nearly 2 weeks. As sampling progressed, we improved our sampling system and methods. A Seabird CTD SBE-37 was added in 2000. Thus, most of the data presented herein were obtained in the

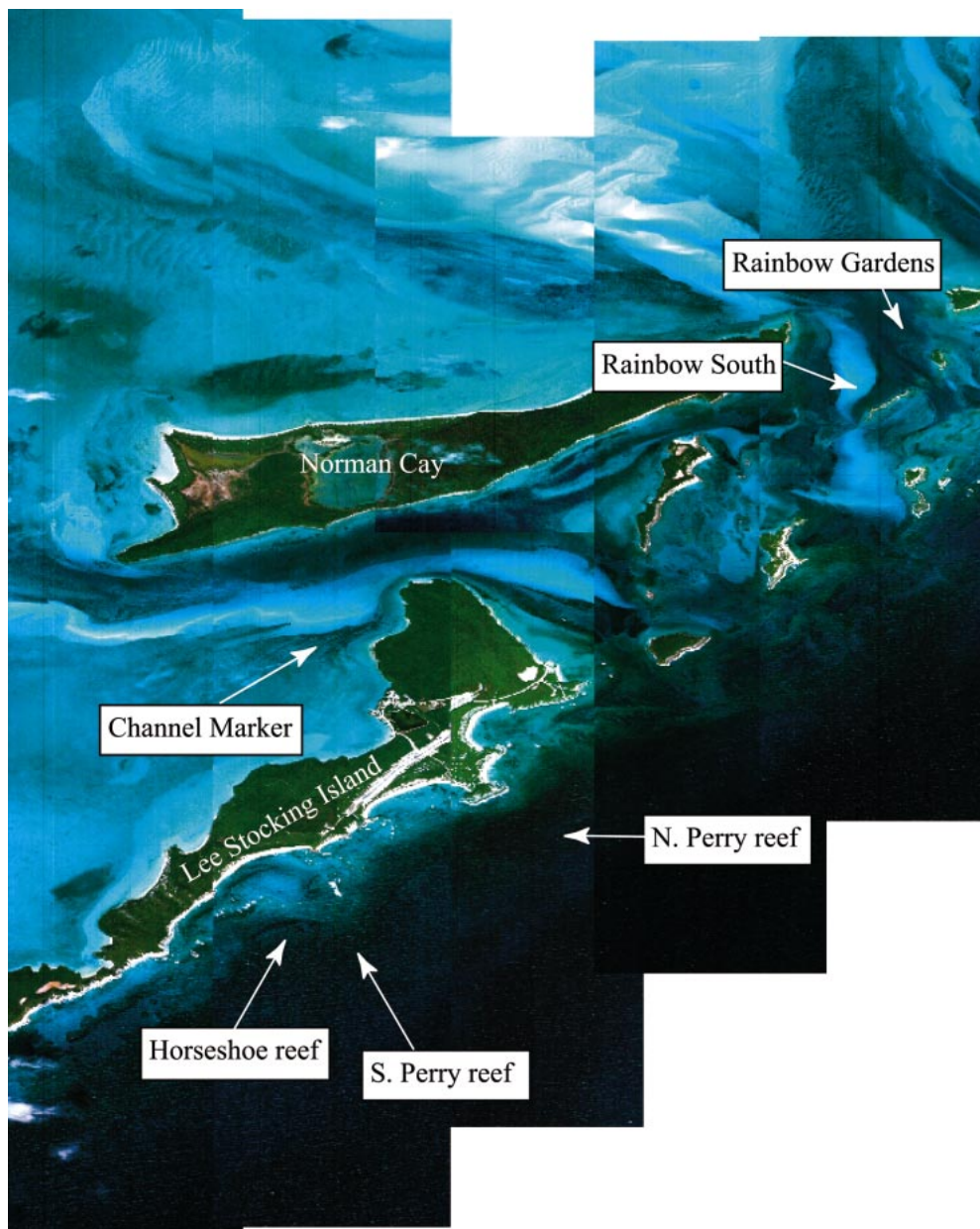


Fig. 1. The location of the sampling sites. Rainbow Garden, Rainbow South, and Channel Marker are on shallow banks, whereas Horseshoe, North and South Perry reefs are deeper and face Exuma Sound to the east of Lee Stocking Island, Bahamas. (Remote sensing image courtesy of Dr. C. Davis of Naval Research Laboratory, Washington, DC.)

spring of 2000. Given the limited observation time, these data do not provide a climatology of the optical variability at the sites (e.g., we did not sample during the hurricane season). We did, however, measure at different phases of the tides as well as at night.

Properties presented—Because we cannot present the total of the optical measurements, we concentrate herein on a fraction of the optical measurements. Below we summarize the optical properties analyzed and their biogeochemical interpretation.

Measured properties:

1. $a_g(440)$ [or $c_g(440)$] denotes the absorption (or attenuation) by colored dissolved material (CDM). In the coastal ocean, CDM absorption is an indicator of the concentration of dissolved organic material, although the exact relationship varies between environments (Blough and Del Vecchio in press). In this article, it is denoted by a_g or c_g . In the water column, the two were equal in our measurements. For pore-water measurements, we present only absorption data because the attenuation was always significantly higher, probably because of scattering by colloids.
2. $c_{pg}(650)$ is an indicator of total suspended particulate

Table 1. Location, date, local time, height above bottom (HAB), substrate type, and optical property obtained from transects above bottom (see method section). Property values are for the median, except when denoted by angle brackets for mean or an underline for the absolute deviation. Data from the sections at SP and HS from May 2000 are averages of multiple transects (V and W sampling patterns).

Station	Date	Time	HAB (cm)	Substrate	a_g	a_g	a_g	s	[Chl]	$\langle \text{Chl} \rangle$	$\frac{[\text{chl}]}{[\text{Chl}]}$	c_{pg}	$\langle c_{pg} \rangle$	$\frac{c_{pg}}{c_{pg}}$	γ	$\langle \gamma \rangle$
HS	25 May 99	1000	10	Reef	0.051	0.002	0.013	0.013	0.01	0.07	0.02	0.071	0.110	0.072	1.06	0.82
HS	25 May 99	1000	10	Sand	0.052	0.001	0.013	0.013	0.00	-0.01	0.00	0.068	0.069	0.006	1.17	1.16
NP	26 May 99	1030	10	Reef	0.043	0.001	0.013	0.013	0.03	0.17	1.27	0.082	0.143	0.111	1.07	0.68
NP	26 May 99	1030	10	Sand	0.042	0.001	0.013	0.013	0.04	0.04	0.26	0.088	0.089	0.004	1.02	1.01
HS	10 Jan 00	1000	10	Reef	0.019	0.003	0.026	0.026	-0.09	-0.07	0.01	0.059	0.060	0.005	1.07	1.07
HS	10 Jan 00	1000	10	Sand	0.017	0.002	0.028	0.028	-0.05	-0.03	0.01	0.062	0.062	0.003	1.08	1.08
SP	11 Jan 00	830	10	Reef	0.028	0.003	0.016	0.016	0.01	0.03	0.00	0.059	0.059	0.003	1.11	1.10
SP	11 Jan 00	830	10	Sand	0.028	0.004	0.015	0.015	0.03	0.02	0.00	0.069	0.069	0.003	1.08	1.07
SP	15 May 00	1000	10	Reef	0.029	1.394	0.013	0.013	0.15	0.12	0.61	0.089	0.090	0.006	0.85	0.81
SP	15 May 00	1000	10	Sand	0.023	0.068	0.014	0.014	0.17	0.19	0.55	0.108	0.108	0.005	0.65	0.66
SP	15 May 00	2030	10	Reef	0.035	0.006	0.014	0.014	0.09	0.15	0.92	0.092	0.093	0.008	0.93	0.88
SP	15 May 00	2030	10	Sand	0.023	0.002	0.016	0.016	0.15	0.15	0.38	0.118	0.118	0.007	0.62	0.64
SP	16 May 00	1030	10	Reef	0.028	0.010	0.014	0.014	0.13	0.09	1.77	0.095	0.104	0.020	0.82	0.82
SP	16 May 00	1030	10	Sand	0.024	0.002	0.016	0.016	0.17	0.18	0.50	0.110	0.111	0.006	0.72	0.72
SP	16 May 00	2030	10	Reef	0.036	0.008	0.013	0.013	0.07	0.07	0.55	0.097	0.097	0.010	1.00	0.99
SP	16 May 00	2030	10	Sand	0.025	0.004	0.014	0.014	0.14	0.15	0.47	0.115	0.116	0.008	0.75	0.73
HS	17 May 00	2100	10	Reef	0.067	0.005	0.009	0.009	0.09	0.09	0.52	0.125	0.126	0.009	0.90	0.88
HS	17 May 00	2100	10	Sand	0.057	0.022	0.011	0.011	0.22	0.21	0.51	0.167	0.162	0.014	0.56	0.59
HS	22 May 00	930	10	Reef	0.046	0.006	0.014	0.014	0.32	0.28	0.27	0.065	0.066	0.003	1.32	1.31
HS	22 May 00	930	10	Sand	0.044	0.001	0.014	0.014	0.30	0.27	0.37	0.069	0.070	0.003	1.29	1.28
HS	25 May 99	1000	50	Reef	0.047	0.002	0.014	0.014	0.01	-0.01	0.00	0.071	0.071	0.006	1.12	1.11
HS	25 May 99	1000	50	Sand	0.048	0.001	0.014	0.014	-0.01	0.00	0.00	0.074	0.074	0.004	1.08	1.07
HS	10 Jan 00	1000	100	Reef	0.017	0.002	0.027	0.027	-0.05	-0.03	0.01	0.064	0.064	0.003	1.04	1.04
HS	10 Jan 00	1000	100	Sand	0.017	0.002	0.028	0.028	-0.03	-0.02	0.01	0.063	0.063	0.003	1.07	1.06
SP	11 Jan 00	830	100	Reef	0.027	0.002	0.018	0.018	0.05	0.05	0.00	0.061	0.062	0.003	1.09	1.09
SP	11 Jan 00	830	100	Sand	0.026	0.002	0.018	0.018	0.04	0.05	0.00	0.068	0.068	0.003	1.08	1.08
HS	17 May 00	2100	100	Reef	0.063	0.002	0.012	0.012	0.09	0.11	0.42	0.148	0.149	0.013	0.60	0.60
HS	17 May 00	2100	100	Sand	0.056	0.002	0.013	0.013	0.18	0.18	0.44	0.166	0.162	0.013	0.51	0.55
SP	11 Jan 00	830	200	Reef	0.028	0.002	0.018	0.018	0.03	0.03	0.00	0.065	0.066	0.003	1.08	1.08
SP	11 Jan 00	830	200	Sand	0.027	0.002	0.018	0.018	0.04	0.04	0.00	0.068	0.069	0.003	1.07	1.07

mass (volume or concentration, e.g., Spinrad et al. 1983; CDM absorption at this wavelength is negligible). To a lesser degree, it also varies with size distribution and composition. In this article, it is denoted as c_{pg} .

Derived properties:

1. $[\text{chl}] \approx [a_{pg}(676) - a_{pg}(650)]/0.014$ is an indicator of chlorophyll *a* concentration (in $\mu\text{g L}^{-1}$), which in turn is an indicator, at a given light level, of phytoplankton biomass. The equation above was found to correlate very well with fluorometric determination of chlorophyll (Roesler pers. comm.). Note that when very little [chl] is present relative to detritus, this estimate may be negative, which reflects the decrease of absorption with wavelength typical of detritus.
2. γ is the slope of c_p , an indicator of tendencies of the particulate size distribution (Boss et al. 2001*b,c*). The parameter γ will be larger when the sample is dominated by small particles. This parameter is obtained by a nonlinear least-squares fit to the data of a relationship with the form

$$c_p = \tilde{c}_p(\lambda_0) \left(\frac{\lambda}{\lambda_0} \right)^{-\gamma}$$

Note that γ does not depend on the reference wavelength, λ_0 .

3. s is the slope of a_g , indicator of CDM “flavor.” A steep slope (~ 0.02) represents “fulvic”-like or low-molecular-weight material, whereas a smaller slope (~ 0.01) represents “humic”-like or high-molecular-weight material (Carder et al. 1989; Blough and Del Vecchio in press). The spectral slope, s , is obtained by nonlinear least-squares fit to the data of a relationship with the form

$$a_g = \bar{a}_g(\lambda_0) \exp[-s(\lambda - \lambda_0)]$$

Note that s does not depend on λ_0 .

We quantify the concentration or “amount” of each measured property using its mean (denoted by angle brackets) and median. The mean will be influenced by rare big particles, whereas the median will not. The difference between the mean and median of particulate properties provides a measure of large rare particles passing through the AC-9, because they cause positive spikes. Variability in each property is also quantified by the mean absolute deviation (denoted by an underline), a more robust estimator of variability than the standard deviation (Press et al. 1992). It is defined as

$$\underline{a} \equiv \frac{1}{N} \sum_{i=1}^N |a_i - \langle a \rangle|$$

where a_i denotes the i th measurement of parameter a and $\langle a \rangle$ denotes its mean.

Errors and confidence interval—Errors in absorption and attenuation that are due to calibration are assumed to be $< O(0.005 \text{ m}^{-1})$. The calibration errors cancel when particulate properties are considered, because we subtracted two measurements (with and without filter) to obtain them. Instrumental noise is $O(0.001 \text{ m}^{-1})$ (Twardowski et al. 1999) and is amplified (by $\sqrt{2}$) for particulate properties. Note,

however, that the dissolved and total measurements are not carried out simultaneously (but usually within 5 min of each other); thus, errors due to temporal aliasing may be present in the particulate measurement. Spectral slopes of CDM and particulate beam attenuation are significant to $O(10\%$ and 5% , respectively) (based on bootstrap method, e.g., Press et al. 1992, p. 691). On the basis of the uncertainty in absorption, [chl] is significant to within $0.35 \mu\text{g L}^{-1}$ which is usually much larger than the signal measured. However, when comparing spectral slopes, absorption (and [chl] estimates), and attenuation values between measurements performed in a single dive, the differences in measurements between two depths or two substrates are significant at a much lower level, because instrument calibration is unlikely to change during a dive. For a homogeneous sample, the error estimate of a single measurement needs to be divided by the square root of the number of independent observations (e.g., Press et al. 1992). Measurements were taken at 6 Hz for $O(2\text{--}10)$ min with a sample volume of $O(20)$ ml and pumped at $2\text{--}6 \text{ L min}^{-1}$, which resulted in the number of independent observations per transect being >150 .

Measured currents at the sites—The current velocity fields at NP and RS were measured by Dr. Rob Wheatcroft (unpubl. data). At NP, the largest velocity was along the reef, following the bathymetry. Across-reef velocities had a mean absolute velocity of 0.2 cm s^{-1} , a standard deviation of 3.5 cm s^{-1} , and a maximum velocity of 20 cm s^{-1} . Thus, most of the time there was little exchange of water between reef and sand flats, except for short episodic exchanges that were probably associated with stresses due to large swells (whose direction was often across the reef/sand boundary). At RS, tidal velocities were $O(40 \text{ cm s}^{-1})$. These tended to homogenize the waters over the shallow banks.

Results

Horizontal gradients in optical properties across coral-sand boundaries—Results from fifteen transects carried out between 10 and 200 cm above the bottom at both reefs and adjacent sand flats at three different sites (NP, SP, and HS) are presented in Table 1. An example of a record measured during one of the transects is presented in Fig. 2. In Table 2, we summarize the number of transects (out of a total of 15) for which a given property was either larger over the reef or over a nearby sand flat.

These results can be summarized as follows:

1. The variability in all properties was larger over the reef.
2. CDM concentration was larger over the reef.
3. Attenuation was larger over sand, but its spectral slope was larger over the reef.
4. In most cases, [chl] was larger over sand.

In addition, we observed that the mean of a given property was, in general, higher than its median. The slope of the CDM was not significantly different between the two substrates. In contrast to the gradients observed on the Exuma Sound side of LSI, we did not measure horizontal and vertical gradients in optical properties over the banks (RG and CM) that were larger than the local temporal gradients over scales of minutes (data not shown).

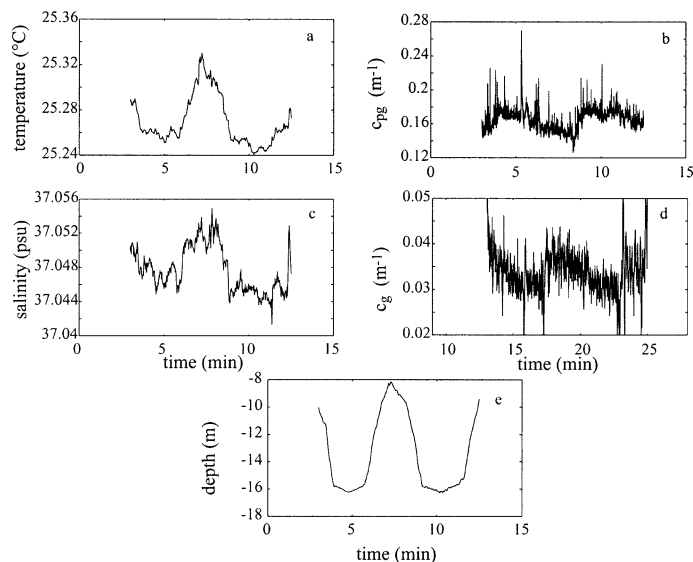


Fig. 2. Typical distributions of physical and optical properties obtained along a transect at a height of 10 cm above the bottom at South Perry reef (15 May 2000). The pattern sampled was a “W” string pattern laid earlier on the bottom. Properties displayed are (a) temperature, (b) attenuation at 650 nm, (c) salinity, (d) dissolved attenuation at 440 (similar to absorption), and (e) depth of diver. The dissolved measurement took place at the same location immediately after the measurement without the filter. Below 15.7 m, the bottom substrate was sand, whereas above it the substrate consisted of a mixture of coral, sponges, and macroalgae.

Vertical gradients in optical properties above reef and sand—In Table 3, we summarize values of properties obtained at different depths above reef and sand and from which vertical gradient could be inferred. In Table 4, the number of occurrences where the value at 10 cm was larger than the value at a depth above it is displayed for each type sand and reef.

These results can be summarized as follows:

1. The variability in all properties was larger at 10 cm above both reef and sand than further away from the bottom.
2. The CDM concentration was larger at 10 cm above the bottom than further from the bottom. The CDM spectral slope was smaller at 10 cm above both reef and sand.
3. Attenuation increased above the reef, whereas above sand, the change in concentration was not significant.
4. The attenuation spectral slope decreased with increasing distance from both sand and reef substrate.
5. [chl] increased away from substrate.

A comparison of transects above seagrass and shallow coral reef (RG and CM) showed no significant vertical gradients (data not shown). CDM gradients near CM are presented in the next section.

Gradients in CDM between pore waters and overlying waters—Using a rigid attachment to the intake tube (see Zaneveld et al. 2001), we measured the CDM absorption within and above the sediment in three different types of sediment all located within 150 m of each other near CM. Although our method of sampling was far from perfect, in particular in that it required a relatively large volume of water, it provided the direction of gradients between the sediment pore waters and the overlying waters (Fig. 3). These observations were consistent in the direction of gradient compared with CDM fluorescence measurements of Dr. D. Burdige at the same sites (D. Burdige pers. comm.). During flood tide, we found all bottoms, varying from dense grass beds to sparse grass beds to barren carbonate sediments composed of ooids, to have higher CDM absorption than the overlying waters. During ebb tide, the barren ooids bottom was the only type to have less CDM absorption than the overlying waters (Fig. 3). No significant differences were found in CDM spectral slope across the sediment water interface (not shown). Similar gradients were observed during January and May 2000 (e.g., Zaneveld et al. 2001).

Gradients in CDM between banks and Exuma Sound—A time series in hydrographic and optical properties was obtained at RS during 20–21 May 2000 at 50 cm above the bottom (average bottom depth, 3 m). RS is a tidally flushed channel that connects the banks with Exuma Sound (Fig. 1). Fluxes of CDM were mostly negative (Fig. 4d), which implies that the banks were, on average, exporting CDM to the sound. CDM concentration, its spectral slope, and the water salinity were higher over the bank water relative to Exuma water (Fig. 4). The correlation between salinity and CDM was high ($R^2 = 0.95$) and positive (Fig. 4e).

Discussion

Over timescales of minutes and horizontal scales of tens of meters, observable horizontal gradients between reefs and adjacent sand flats and observable vertical gradients above the reef and sand flats were found on the Exuma Sound side of LSI (NP, SP, and HS). Over the bank (CM and RG), it was not possible to distinguish temporal gradients from spatial gradients of all properties [except at distances of $O(10)$ cm) from the bottom, Fig. 3]. We believe the above differences between the two environments to be due to the difference in current velocities (and, hence, mixing) between both environments.

Processes associated with the bottom substrate create larger variability in particulate and dissolved properties relative to higher up in the water column (Table 4). This is consistent with biogeochemical processes associated with the substrate being sources or sinks for particulate and dissolved material. Variability is higher over the reef relative to sand (Table 2),

Table 2. Number of observations (out of 15) for which each property was higher above the reef or sand. Based on data in Table 1.

	a_g	$\underline{a_g}$	s	[chl]	$\langle \text{chl} \rangle$	$\underline{[chl]}$	c_{PE}	$\langle c_{\text{PE}} \rangle$	$\underline{c_{\text{PE}}}$	γ	$\langle \gamma \rangle$
Reef/sand	13/2	12/3	6/9	4/11	6/9	12/3	2/13	3/12	11/4	12/3	11/4

Table 3. Location, date, local time, height above bottom (HAB), substrate type, and optical property obtained from transects at difference distances above bottom at the same location (see Materials and method section). Property values are for the median, except when denoted by angle brackets for mean or an underline for the absolute deviation. Data from the sections at SP and HS from May 2000 are averages of multiple transects (V and W sampling patterns).

Station	Date	Time	HAB (cm)	Substrate	a_g	a_g	s	[chl]	<chl>	[chl]	c_{pg}	< c_{pg} >	c_{pg}	γ	< γ >
HS	25 May 99	1000	10	Reef	0.051	0.002	0.013	0.01	0.07	0.02	0.071	0.110	0.072	1.06	0.82
HS	25 May 99	1000	50	Reef	0.047	0.002	0.014	0.01	-0.01	0.00	0.071	0.071	0.006	1.12	1.11
HS	10 Jan 00	1000	10	Reef	0.019	0.003	0.026	-0.09	-0.07	0.01	0.059	0.060	0.005	1.07	1.07
HS	10 Jan 00	1000	100	Reef	0.017	0.002	0.027	-0.05	-0.03	0.01	0.064	0.064	0.003	1.04	1.04
SP	11 Jan 00	830	10	Reef	0.028	0.003	0.016	0.01	0.03	0.00	0.059	0.059	0.003	1.11	1.10
SP	11 Jan 00	830	100	Reef	0.027	0.002	0.018	0.05	0.05	0.00	0.061	0.062	0.003	1.09	1.09
SP	11 Jan 00	830	200	Reef	0.028	0.002	0.018	0.03	0.03	0.00	0.065	0.066	0.003	1.08	1.08
HS	17 May 00	2100	10	Reef	0.067	0.005	0.009	0.09	0.09	0.52	0.125	0.126	0.009	0.90	0.88
HS	17 May 00	2100	100	Reef	0.063	0.002	0.012	0.09	0.11	0.42	0.148	0.149	0.013	0.60	0.60
NP	22 May 00	1045	10	Reef	0.033	0.315	0.012	-0.12	-0.11	0.16	0.069	0.069	0.004	1.42	1.39
NP	22 May 00	1045	100	Reef	0.030	0.078	0.014	0.04	0.04	0.12	0.075	0.075	0.003	0.95	0.96
HS	25 May 99	1000	10	Sand	0.052	0.001	0.013	0.00	-0.01	0.00	0.068	0.069	0.006	1.17	1.16
HS	25 May 99	1000	50	Sand	0.048	0.001	0.014	-0.01	0.00	0.00	0.074	0.074	0.004	1.08	1.07
HS	10 Jan 00	1000	10	Sand	0.017	0.002	0.028	-0.05	-0.03	0.01	0.062	0.062	0.003	1.08	1.08
HS	10 Jan 00	1000	100	Sand	0.017	0.002	0.028	-0.03	-0.02	0.01	0.063	0.063	0.003	1.07	1.07
SP	11 Jan 00	830	10	Sand	0.028	0.004	0.015	0.03	0.02	0.00	0.069	0.069	0.003	1.08	1.06
SP	11 Jan 00	830	100	Sand	0.026	0.002	0.018	0.04	0.05	0.00	0.068	0.068	0.003	1.08	1.08
SP	11 Jan 00	830	200	Sand	0.027	0.002	0.018	0.04	0.04	0.00	0.068	0.069	0.003	1.07	1.07
HS	17 May 00	2100	10	Sand	0.057	0.022	0.011	0.22	0.21	0.51	0.167	0.162	0.014	0.56	0.59
HS	17 May 00	2100	100	Sand	0.056	0.002	0.013	0.18	0.18	0.44	0.166	0.162	0.013	0.51	0.55
RG	27 May 99	1630	10	Sand	0.046	0.002	0.013	-0.02	-0.02	0.01	0.103	0.112	0.016	0.95	0.88
RG	27 May 99	1630	50	Sand	0.041	0.002	0.015	-0.02	-0.01	0.00	0.101	0.102	0.003	0.95	0.95

Table 4. Number of observations for which each property was higher at 10 cm versus higher up in the water column (50, 100, or 200 cm). Based on data in Table 3.

	a_g	$\underline{a_g}$	s	[chl]	$\langle \text{chl} \rangle$	$\underline{[chl]}$	c_{pg}	$\langle c_{pg} \rangle$	$\underline{c_{pg}}$	γ	$\langle \gamma \rangle$
Reef	6/0	6/0	0/6	2/4	2/4	4/2	1/5	1/5	4/2	5/1	5/1
Sand	5/0	5/0	0/5	2/3	1/4	4/1	3/2	3/2	4/1	4/1	4/1

most likely because of the heterogeneity of the reef in both topography and organisms relative to the sand flat. This heterogeneity results in small-scale flow patterns (Abelson et al. 1993). In addition, fish activity over reefs has been found to be an important source of variability (Yahel et al. 2002).

We find reefs and seagrass beds to be sources of dissolved material. This CDM pattern is likely to be due to release of metabolites from sponges and corals and/or byproducts of primary production by the microalgae on the reef. Dense seagrass beds are associated at CM with large mats of decomposing dead leaves, which are likely to be the major source of the CDM released over the bank. CDM released by reef has a lower spectral slope than the water column above it (Table 4). CDM released by seagrass beds has a higher spectral slope than the Exuma Sound waters (Fig. 4), although this slope is relatively low compared with coastal CDM (where $s \sim 0.015$, Roesler et al. 1989). Low spectral slope is characteristic of humic substances which have relatively high molecular weight (Carder et al. 1989; Blough and Del Vecchio in press).

Above reefs, in general, there was less particulate material than higher up in the water column or in the adjacent sand flats. The [chl] pattern observed was consistent with the removal of [chl]-containing particles just above the reef, which is probably associated with removal of phytoplankton by the benthic fauna, as has been observed in other reef systems (Yahel et al. 1998).

The particulate attenuation decrease towards the bottom was associated with *steepening* of the attenuation spectral slope, which suggests that near the substrate there was removal of the relatively bigger particles compared with higher up in the water column. This gradient has the opposite sign of the gradient in attenuation spectral slope observed when

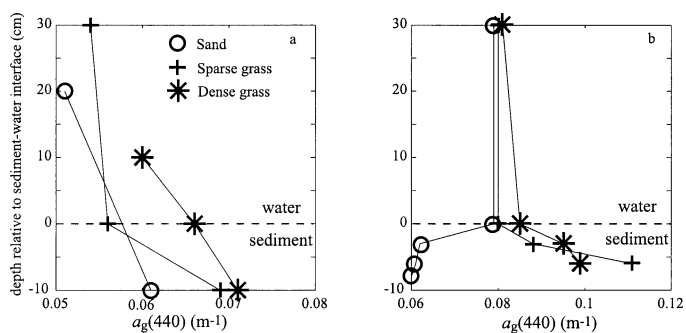


Fig. 3. CDM concentration across the sediment water boundary at Channel Marker at (a) flood tide (30 May 1999) and (b) ebb tide (31 May 1999) in three types of bottom substrate located at a horizontal distance <150 m from each other. Measurements were performed within 45 min and contain between two and four replicates. Maximum absolute deviation at a given depth was 0.003 m^{-1} .

particulates are resuspended (Boss et al. 2001b); resuspension and settling of particulate material result in *flattening* of the attenuation spectral slope toward the bottom. Note that even above the sand flat, we observed steepening of the spectral slope toward the bottom, which suggests that benthic organisms within the sand filter out particles from the water adjacent to the substrate. Removal of large particles is consistent with the [chl] decrease above the reef as phytoplankton are optically “large.”

Grass-covered sediment are found to be sources of CDM to the water column, whereas ooids sediment (which are poor in organic content) have a CDM gradient across the sediment water interface that depends on the phase of the tide. This reversal suggests that the CDM absorption in the ooids was due to slow diffusional flux into and out of the sediment.

This local, substrate related source of CDM created a large-scale gradient of CDM absorption between the banks and Exuma Sound (Fig. 4). Because more evaporation occurs over the banks, the correlation of salinity and CDM absorption is positive, in contrast to the negative correlation found between salinity and CDM in coastal waters affected by fluvial inputs (e.g., Blough and Del Vecchio in press). Fluxes of CDM and its associated absorption from sediment pore waters to the water column have been hypothesized elsewhere to occur over the continental shelf (Boss et al. 2001a) and were observed here.

Near-bottom optical properties and their variability are im-

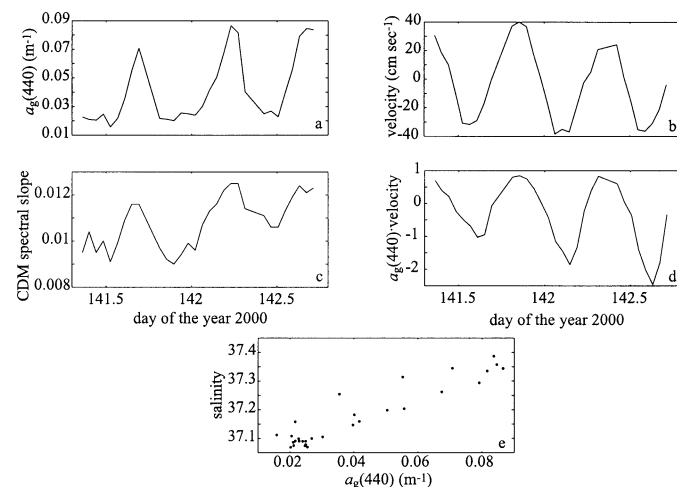


Fig. 4. Once an hour time series of (a) CDM absorption, (b) CDM absorption spectral slope, (c) across-bank velocity (positive towards the shallow banks), (d) across-bank CDM absorption flux per unit area obtained at Rainbow South, and (e) salinity-CDM absorption distribution.

portant inputs into radiative-transfer models that describe light propagation in the coastal ocean. Imaging of bottom structures, flora, and fauna depends on the near-bottom optical properties. The results presented herein (Tables 1, 2) suggest that near-bottom variability in IOPs is usually small, although significant. The mean attenuation coefficient in the blue could vary by 50% between reef and sand (*see also* fig. 4 of Zaneveld et al. 2001). However, further up in the water column the differences diminish, consistent with the sources of variability being close to the substrate.

It can be shown that in a heterogeneous environment, such as the near-bottom environment, a sensor will be affected by the mean of the optical properties of the medium (rather than the median or mode). As seen here (*see also* fig. 4 of Zaneveld et al. 2001), near the bottom, the mean of attenuation can be tens of percents larger than the median, which indicates the importance of sampling at scales that encompass the local variability of interest.

We have shown that the near-bottom optical properties are influenced by the type of bottom present, which reflects the biogeochemical processes associated with each particular benthic environment. The change in IOP can be significant and may need to be taken into account in radiative transfer calculations.

In addition, we suggest that local benthic processes can result in large-scale gradients between environments as observed in CDM absorption between the bank waters and the adjacent Exuma Sound.

In situ optical measurements have seldom been used to quantify biogeochemical processes. Our results suggest that optical measurements are sensitive enough to infer biogeochemical processes associated with bottom substrates.

References

- ABELSON, A., T. MILOH, AND Y. LOYA. 1993. Flow patterns induced by substrata and body morphologies of benthic organisms, and their roles in determining availability of food particles. *Limnol. Oceanogr.* **38**: 1116–1124.
- BLOUGH, N. V., AND R. DEL VECCHIO. 2002. Distribution and dynamics of chromophoric dissolved organic matter (CDOM) in the coastal environment, p. 509–546. *In* D. Hansell and C. Carlson [eds.], *Biogeochemistry of marine dissolved organic matter*. Academic.
- BOSS, E., AND OTHERS. 2001a. Spectral particulate attenuation and particle size distribution in the bottom boundary layer of a continental shelf. *J. Geophys. Res.* **106**: 9509–9516.
- , ———, J. R. V. ZANEVELD, AND A. H. BARNARD. 2001b. Spatial and temporal variability of absorption by dissolved material at a continental shelf. *J. Geophys. Res.* **106**: 9499–9508.
- , M. S. TWARDOWSKI, AND S. HERRING. 2001c. Shape of the particulate beam attenuation spectrum and its inversion to obtain the shape of the particulate size distribution. *Appl. Opt.* **40**: 4885–4893.
- BRAINERD, K. E., AND M. C. GREGG. 1995. Surface mixed and mixing layer depths. *Deep-Sea Res.* **42**: 1521–1543.
- CARDER, K. L., R. G. STEWARD, G. R. HARVEY, AND P. B. ORTNER. 1989. Marine humic and fulvic acids: Their effects on remote sensing of ocean chlorophyll. *Limnol. Oceanogr.* **34**: 68–81.
- , C.-C. LIU, Z. LEE, D. C. ENGLISH, J. PATTEN, F. R. CHEN, J. E. IVEY, AND C. O. DAVIS. 2003. Illumination and turbidity effects on observing faceted bottom elements with uniform Lambertian albedos. *Limnol. Oceanogr.* **48**: 355–363.
- DAGG, M. J. 1997. Vertical migration and feeding behaviour of *Calanus pacificus* females during a phytoplankton bloom in Dabob Bay, U. S. *Limnol. Oceanogr.* **42**: 974–980.
- DUBINSKY, Z. [ED.]. 1990. *Coral reefs*. Elsevier.
- EREZ, J. 1990. On the importance of food sources in coral reef ecosystems, p. 411–418. *In* Z. Dubinsky [ed.], *Coral reefs*. Elsevier.
- FRECHETTE, M., C. A. BUTMAN, AND W. R. GEYER. 1989. The importance of boundary-layer flows in supplying phytoplankton to the benthic suspension feeder, *Mytilus edulis* L. *Limnol. Oceanogr.* **34**: 19–36.
- HEAP, A. D., P. LARCOMBE, AND K. J. WOOLFE. 1999. Storm-dominated sedimentation in a protected basin fringed by coral reefs, Nara Inlet, Whitsunday Islands, Great Barrier Reef, Australia. *Aust. J. Earth Sci.* **46**: 443–451.
- HICKEY, B. M., P. MACCREADY, E. ELLIOTT, AND N. B. KACHEL. 2000. Dense saline plumes in Exuma Sound, Bahamas. *J. Geophys. Res.* **105**: 11471–11488.
- LARCOMBE, P., P. V. RIDD, A. PRYTZ AND B. WILSON. 1995. Factors controlling suspended sediment on inner-shelf coral reefs, Townsville, Australia. *Coral Reefs* **14**: 163–171.
- , AND K. J. WOOLFE. 1999. Terrigenous sediments as influences upon Holocene nearshore coral reefs, central Great Barrier Reef, Australia. *Aust. J. Earth Sci.* **46**: 141–154.
- LEE, Z. K. L., C. D. MOBLEY, R. G. STEWARD, AND J. S. PATCH. 1999. Hyperspectral remote sensing for shallow waters: 2. Deriving bottom depths and water properties by optimization. *Appl. Opt.* **38**: 3831–3843.
- MCLEAN, E. A., H. R. BURRIS JR., AND M. P. STRAND. 1995. Short-pulse range-gated optical imaging in turbid water. *Appl. Opt.* **34**: 4343–4351.
- MIDDLETON, G. V., AND J. B. SOUTHARD. 1984. *Mechanics of sediment movement*, 2nd ed. SEPM.
- PAK, H. 1983. Fluctuation of beam-attenuation coefficient in the lowest 2m on the continental rise off Nova Scotia. *Mar. Geol.* **51**: 77–97.
- PREISENDORFER, R. W. 1976. *Hydrologic optics*. Pacific Marine Environment Lab/NOAA.
- PRESS, W. H., S. A. TEUKOLSKY, W. T. VETTERLING, AND B. P. FLANNERY. 1992. *Numerical recipes in C*, 2nd ed. Cambridge Univ. Press.
- ROESLER, C. S., M. J. PERRY, AND K. L. CARDER. 1989. Modeling in situ phytoplankton absorption from total absorption spectra in productive inland marine waters. *Limnol. Oceanogr.* **34**: 1510–1523.
- SPINRAD, R. W., J. R. V. ZANEVELD, AND J. C. KITCHEN. 1983. A study of the optical characteristics of the suspended particles in the benthic nepheloid layer of the Scotian rise. *J. Geophys. Res.* **88**: 7641–7645.
- TWARDOWSKI, M. S., J. M. SULLIVAN, P. L. DUNAGHAY, AND J. R. V. ZANEVELD. 1999. Microscale quantification of the absorption by dissolved and particulate material in coastal waters with an AC-9. *J. Atmos. Ocean. Tech.* **16**: 691–707.
- YAHIEL, G., A. F. POST, K. FABRICIUS, D. MARIE, D. VAULOT, AND A. GENIN. 1998. Phytoplankton distribution and grazing near coral reefs. *Limnol. Oceanogr.* **43**: 551–563.
- , G. YAHIEL, AND A. GENIN. 2002. Daily cycles of suspended sand at coral reefs: A biological control. *Limnol. Oceanogr.* **47**: 1071–1083.
- ZANEVELD, J. R. V., E. BOSS, AND C. M. MOORE. 2001. A diver-operated optical and physical profiling system. *J. Atmos. Ocean. Tech.* **18**: 1421–1427.

Received: 28 September 2001

Accepted: 3 April 2002

Amended: 25 April 2002